

An Adjacent Dibenzotetraazaporphyrin: A Structural Intermediate between Tetraazaporphyrin and Phthalocyanine

Nagao Kobayashi,^{*,†} Hideya Miwa,[†] Hiroaki Isago,[‡] and Tatsuya Tomura[§]

Department of Chemistry, Graduate School of Science, Tohoku University, Sendai 980-8578, Japan, National Research Institute for Metals, 1-2-1 Sengen, Tsukuba, Ibaraki 305-0047, Japan, and R & D Center, Ricoh Co. Ltd., Shin-ei-cho 16-1, Tsuzuki-ku, Yokohama 224-0035, Japan

Received June 10, 1998

An *adjacent* dibenzotetraazaporphyrin, in which two benzene units are fused to the adjacent pyrrole rings of tetraazaporphyrin skeleton, has been synthesized as a copper complex for the first time and characterized by electronic absorption and magnetic circular dichroism spectroscopy, by cyclic voltammetry and spectroelectrochemistry using an optically transparent thin layer electrochemical cell. The results were compared with those of tetraazaporphyrin and phthalocyanine analogues. The title compound shows intermediate characteristics between those of normal tetraazaporphyrins and phthalocyanines; the Q-band shifts to the red and becomes more intense while the Soret band broadens with increasing the size of the π -system. With the expansion of the π -system, the first reduction potential does not change significantly, while the first oxidation potential shifts negatively, indicating that the LUMO level remains almost constant while the HOMO level destabilizes significantly. These spectroscopic properties and redox potentials were reproduced by molecular orbital calculations within the framework of the Pariser–Parr–Pople approximation. Thermogravimetry analysis suggests that the skeleton of the adjacent dibenzotetraazaporphyrin complex decomposes at about 95 degrees lower than that of the tetra-*tert*-butylated phthalocyanine analogue.

Introduction

Phthalocyanines (Pcs) offer a unique chemistry with a great many possible industrial applications.^{1,2} Because of their easy synthesis, high stability, the presence of intense π – π^* transitions in the visible region and their redox activity, they have found use as dyes and pigments, as catalysts for removing sulfur from crude oil, and more recently as the photoconducting agent in photocopiers. Recently there has been renewed interest in the use of Pcs in a variety of high technology fields including semiconductor devices, photovoltaic and solar cells, electrophotography, rectifying devices, molecular electronics, Langmuir–Blodgett films, electrochromic display devices, low-dimensional conductors and synthetic metals, gas sensors, liquid crystals, nonlinear optics, optical disks, and photodynamic cancer therapy and as photosensitizers, electrocatalytic agents, deodorants, and germicides (disinfectants). With the development of laser technology, robust compounds having a principal absorption around 600–650 nm are becoming increasingly important in the fields, for example, of optical disks. In this connection, the absorption of Pcs is too long (roughly ca. 650–730 nm)^{3,4} while those of normal porphyrins not containing *meso*-nitrogens are too short and weak. Accordingly, with respect to the above, we report herein an *adjacent* type dibenzotetraazaporphyrin, **1** (Fig-

ure 1),⁵ which is a structural intermediate between tetraazaporphyrins (TAPs) and Pcs. The π -conjugated system of this compound is smaller than those of Pcs, and, as shown later, the compound has an intense main band (the Q-band) in the desired spectral region, which is strengthened as a result of the superimposition of two transitions.⁶ On the other hand, its structural isomer, the *opposite* dibenzotetraazaporphyrin is not suitable, because this does not have a sufficient intensity in the spectral region due to its split Q-band⁶ (for the same reason, *opposite* dinaphthotetraazaporphyrin shows a split Q-band).⁷

Experimental Section

(i) Measurements. Electronic and FT-IR spectra were measured with a Shimadzu UV-3100 and a JASCO FT/IR-7000 spectrophotometer, respectively. Magnetic circular dichroism (MCD) measurements were made with a JASCO J-400X spectrodichrometer equipped with a JASCO electromagnet that produced magnetic fields up to 1.09 T with parallel and antiparallel fields. Its magnitude was expressed in terms of molar ellipticity per tesla, $[\theta]_M/10^4 \text{ deg mol}^{-1} \text{ dm}^3 \text{ cm}^{-1} \text{ T}^{-1}$. The 400 MHz ¹H NMR spectra were recorded with a JNM-A400 spectrometer using CDCl₃ as solvent.

[†] Tohoku University.

[‡] National Research Institute for Metals.

[§] Ricoh Co., Ltd.

- (1) (a) *Phthalocyanines: Properties and Applications*; Leznoff, C. C., Lever, A. B. P., Eds.; VCH: Weinheim, Germany, 1989, 1993, 1993, and 1996; Vols. I–IV. (b) Moser, F. H.; Thomas, A. L. *The Phthalocyanines*; CRC: Boca Raton, FL, 1983; Vols. I and II. (c) Lever, A. B. P. *Adv. Inorg. Chem. Radiochem.* **1965**, *7*, 27. (d) Simon, J.; Sirlin, C. *Pure Appl. Chem.* **1989**, *61*, 1625. (e) Schultz, H.; Lehmann, H.; Rein, M.; Hanack, M. *Struct. Bond.* **1990**, *74*, 41.
- (2) *Phthalocyanines: Chemistry and Functions*; Shirai, H., Kobayashi, N., Eds.; IPC Publishers: Tokyo, 1997 (in Japanese).

- (3) Kobayashi, N. In *Phthalocyanines: Properties and Applications*; Leznoff, C. C., Lever, A. B. P., Eds.; VCH: Weinheim, Germany, 1993; Vol. II, Chapter 3.
- (4) Luk'yanets E. A. *Electronic Spectra of Phthalocyanines and Related Compounds*; Tcherkassy: Moscow, 1989.
- (5) *Adjacent* substituted phthalocyanines have recently been reported: (a) Noran, K. L. M.; Hu, M.; Leznoff, C. C. *Synlett* **1997**, 593. (b) Hu, M.; Bresseur, N.; Yidiz, S. Z.; van Lier, J. E.; Leznoff, C. C. *J. Med. Chem.* **1998**, *41*, 1789.
- (6) (a) Kobayashi, N.; Konami, H. In *Phthalocyanines: Properties and Applications*; Leznoff, C. C., Lever, A. B. P., Eds.; VCH: Weinheim, Germany, 1996; Vol. IV, Chapter 9. (b) Konami, H.; Ikeda, Y.; Hatano, M.; Mochizuki, K. *Mol. Phys.* **1993**, *80*, 153.
- (7) Kobayashi, N.; Ashida, T.; Osa, T.; Konami, H. *Inorg. Chem.* **1994**, *33*, 1735.

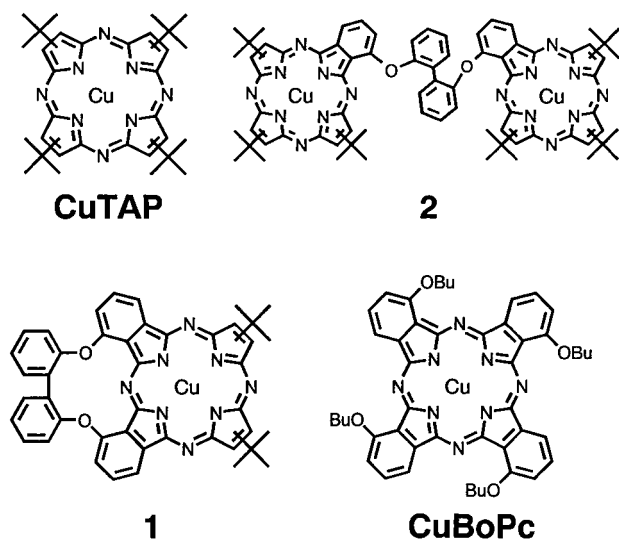


Figure 1. Structures and abbreviations of the compounds that appear in this study.

All of the cyclic voltammetry (CV) experiments were carried out by using a Hokuto Denko HA-501 potentiostat/galvanostat connected to a Hokuto Denko HB-104 function generator and a Rika Denki RY-11 X-Y recorder. In rotating disk electrode voltammetry (RDE) experiments, a Yanaco P10-RE Mk-II disk rotator was used, connected to the above equipment. Conventional three-electrode cells were used, in which a glassy carbon electrode (area = 7.07 mm²) and a platinum wire were used as the working electrode and the auxiliary electrode, respectively. The reference electrode was AgCl/Ag (0.045 V vs SCE⁸ in saturated KCl, separated by a frit) corrected for junction potentials by being referenced internally to the ferrocenium/ferrocene (Fc⁺/Fc) couple. In the solutions used, i.e. in methylene chloride containing 0.1–0.2 M tetrabutylammonium hexafluorophosphate (TBAPF₆), the Fc⁺/Fc couple was observed at approximately 0.40 ± 0.02 V vs AgCl/Ag.⁹ All of the electrochemical experiments were carried out at 25.0 ± 0.5 °C under a dry argon atmosphere. Spectroelectrochemical measurements were carried out using a long-path optically transparent thin layer electrochemical cell (LOTTLE),¹⁰ a Hokuto Denko HA-211 potentiostat/galvanostat, and a Shimadzu UV-160A spectrophotometer.

Thermogravimetry analysis (TGA) and differential thermal analysis (DTA) data were obtained using a Seiko Instruments Inc. SC/5200 system under a nitrogen atmosphere at a heating rate of 10 °C min⁻¹ in 25–500 °C range.

(ii) Synthesis. Different from phthalocyanines, no zinc or nickel tetraazaporphyrins are generally obtained by template reactions.³ Accordingly, these metal-inserted species were not synthesized in this study, although their structures, if present, can be elucidated by NMR spectroscopy. The use of magnesium was possible, and indeed we tried.³ However, the magnesium complexes were not always stable and decomposed to some extent in the course of chromatography using silica gels. Accordingly, we decided to synthesize more stable copper complexes.

Tetra-*tert*-butyltetraazaporphyrinatocopper, CuTAP. This compound was the one we used in our previous paper.¹¹

Tetra-1,8(or 11),15(or 18),22(or 25)-*n*-butyloxyphthalocyaninatocopper, CuBoPc. A mixture of 118 mg of 3-*n*-butyloxyphthalonitrile¹² (58.9 mmol), 38.7 mg of copper (II) dichloride dihydrate (22.7 mmol), 143 mg of urea (2.38 mmol), and a catalytic amount of

ammonium molybdate was heated at 190 °C for 50 min. After cooling to room temperature, crude products were extracted from the reaction mixture and then chromatographed over silica gel using chloroform as eluent. After evaporation of the solvent, CuBoPc was obtained as a dark blue, shining solid in 18.8% yield (24 mg). Anal. Calcd for C₄₈H₄₈N₈O₄Cu: C, 66.69; H, 5.60; N, 12.96. Found: C, 66.32; H, 5.77; N, 12.70.

[2⁴,7¹-(2,2'-Biphenyldioxy)dibenzo[*b,g*]-12(or 13),17(or 18)-di-*tert*-butyl-5,10,15,20-tetraazaporphyrinato(2-)]copper(II), 1. The key point in the synthesis of this compound lies in the preparation of the starting material, i.e. 2,2'-bis(2,3-dicyanophenoxy)biphenyl.¹³ Thus, to a dry DMF solution (150 mL) of 15 g (81 mmol) of 1,1'-biphenyldiol and 6.45 g (60%, 162 mmol) of sodium hydride, which had been cooled to ca. 5 °C, was added 27.9 g (162 mmol) of 3-nitrophthalonitrile dissolved in 150 mL of dry DMF during ca. 1 h under a slow stream of nitrogen. After the addition, the mixture was stirred at room temperature for 48 h and then slowly poured into 450 mL of dilute hydrochloric acid (ca. 0.4 M). From this solution, the crude products were extracted with toluene (1.2 l), and the toluene solution was washed thoroughly 6 times with water. After drying over anhydrous magnesium sulfate, the solvent was evaporated to give a light brown solid. This was purified by column chromatography over silica gel using toluene as eluent (*R_f* = 0.16) and then recrystallization from methanol to give 22.66 g of 2,2'-bis(2,3-dicyanophenoxy)biphenyl as white needles in 64.2% yield, mp 191–192 °C. IR (KBr, cm⁻¹): 3096, 2234 (CN), 1572, 1506, 1460, 1280, 1201, 1114, 1046, 986, 801, 779, 603, 551, 493, 455, 420. ¹H NMR (CDCl₃): δ 7.57–7.61 (d, 2H), 7.40–7.45 (dd, 2H), 7.36–7.39 (dd, 4H), 7.28–7.32 (2H), 7.12–7.14 (2H), 7.05–7.08 (2H).

A 1-chloronaphthalene solution (ca. 30 mL) containing 3.85 g (8.8 mmol) of 2,2'-bis(2,3-dicyanophenoxy)biphenyl, 2.36 g (17.6 mmol) of 1,2-dicyano-3,3-dimethyl-1-butene, and 0.87 g (8.8 mmol) copper(I) chloride was heated to ca. 200 °C, and this temperature was kept constant for 1 day under nitrogen (Scheme 1). After cooling to room temperature, a chloroform-soluble portion alone of the reaction mixture was chromatographed over silica gel using first hexane as eluent. This procedure removed the 1-chloronaphthalene as the reaction solvent. Elution with a mixture of toluene/hexane = 1:1 (v/v) then gave eight fractions with *R_f* values of 0.90, 0.80, 0.70, 0.50, 0.40, 0.31, 0.15, and less than 0.05. Of these eight components, the first three components were individually further chromatographed over silica gel using hexane/chloroform = 5:1 (v/v), giving three components with *R_f* values of (a) 0.83 (purple), (b) 0.60 (purple), and (c) 0.17 (blue). Likewise, the fourth to sixth components were also further chromatographed individually over silica gel using hexane/chloroform = 3:1 (v/v) as eluent to give six fractions with *R_f* values of (d) 0.36 (reddish purple), (e) 0.25 (purple), (f) 0.20 (blue), (g) 0.17 (blue), (h) 0.09 (blue), and (i) 0.01 (blue). From the seventh component, two fractions with *R_f* values of (j) 0.67 (blue) and (k) 0.45 (blue) were obtained by chromatography over silica gel using hexane/chloroform = 1:2 (v/v) as eluent. The eighth component was left as was (l). The approximate amounts of each component and their spectroscopic characteristics are summarized in Table 1. As will be described in detail in the Results and Discussion, the components (i) and (j) were judged to be the desired compound **1** (4.9% yield). Anal. Calcd for C₄₄H₃₄N₈O₂Cu: C, 68.60; H, 4.45; N, 14.55. Found: C, 68.13; H, 4.52; N, 14.19. *m*⁺/*z* 770. IR(KBr, cm⁻¹): 2926, 1736, 1578, 1475, 1394, 1255, 1203, 1137, 1110, 1081, 1054, 1019, 986, 913, 886, 828, 787, 750, 576, 540, 503, 420.

2,2'-Bis{2'-(monobenz[*b*]-7(or 8),12(or 13),17(or 18)tri-*tert*-butyl-5,10,15,20-tetraazaporphyrinyloxy}biphenyl Dicopper(II), 2. This compound was obtained as a byproduct (component (f)) in the synthesis of compound **1**; *m*⁺/*z* 1370. Calcd for C₇₆H₇₄N₁₆O₂Cu₂: 1369.74.

(iii) Computational Method. The **1** and TAP structures were constructed by using phthalocyanine X-ray structural data¹⁴ and by

(8) Bard, A. J.; Faulkner, L. R. *Electrochemical Methods*; John Wiley: New York, 1980.

(9) The position of ferrocenium/ferrocene couple is quite sensitive to the organic solvent employed (see for example ref 17 in: Kobayashi, N.; Lam, H.; Nevin, W. A.; Janda, P.; Leznoff, C. C.; Lever, A. B. P. *Inorg. Chem.* **1990**, 29, 3415).

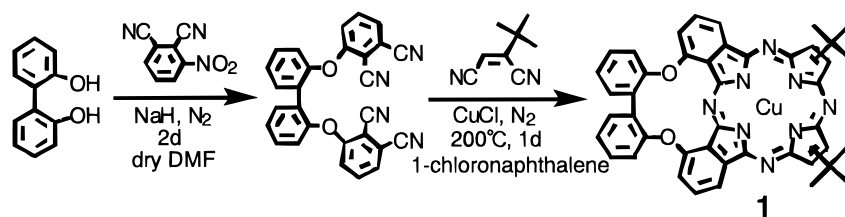
(10) Isago, H.; Kagaya, Y. In *Abstracts of the 74th Annual Meeting of the Chemical Society of Japan*, Kyo-Tanabe, March 27–30, 1998; Abstract No. 4G437.

(11) Kobayashi, N.; Nakajima, S.; Osa, T. *Chem. Lett.* **1992**, 2415.

(12) Kobayashi, N.; Sasaki, N.; Higashi, Y.; Osa, T. *Inorg. Chem.* **1995**, 34, 1636.

(13) Similar types of bisphthalonitriles have been prepared recently for the side-strapped phthalocyanines: Leznoff, C. C.; Drew, D. M. *Can. J. Chem.* **1996**, 74, 307.

Scheme 1

**Table 1.** Components Separated by Chromatography and Their Selected Spectroscopic Data

component	R_f value	eluent	peak position in CHCl_3/nm	relative $\epsilon(Q/\text{Soret})$	Q-bandwidth at half-height/ cm^{-1}	approximate amount/mg	assignment
a (purple)	0.83	H/C ^a 5:1	342, 592	1.48	596.8	10	CuTAP
b (purple)	0.60	H/C 5:1	341, 590	1.47	603.1	50	CuTAP
c (blue)	0.17	H/C 5:1	344, 638	1.95	811.7	15	1
d (reddish purple)	0.37	H/C 3:1	339, 587	1.51	576.3	70	CuTAP
e (purple)	0.25	H/C 3:1	341, 591	1.36	624.2	5	CuTAP
f (blue)	0.20	H/C 3:1	340, 614	1.17	1455.1	trace	2
g (blue)	0.17	H/C 3:1	346, 638	2.58	557.9	95	
h (blue)	0.09	H/C 3:1	346, 641	2.29	585.8	30	
i (blue)	0.01	H/C 3:1	344, 633	2.09	641.2	117	1
j (blue)	0.67	H/C 1:2	340, 632	1.85	956.8	20	1
k (blue)	0.45	H/C 1:2	338, 630, 658, 679	1.14	2465.1	160	Pc ^b
l (blue)	<0.05	H/C 1:1	337, 633, 657, 681	1.13	2502.3	~300	

^a H, hexane; C, chloroform. ^b 1,25:11,15-Bis(2,2'-biphenoxy)phthalocyaninatocopper(II).

making the ring perfectly planar and adopting either C_{2v} (**1**) or D_{4h} (TAP) symmetry. Molecular orbital (MO) calculations were performed for the pyrrole proton-deprotonated dianionic species within the framework of the Pariser–Parr–Pople (PPP) approximation,^{15a} where semiempirical parameters recommended in a recent book^{15b} were employed. These were atomic valence state ionization potentials of 11.16 (carbon), 20.21 (central nitrogen), and 14.12 eV (imino nitrogen), together with atomic valence state electron affinities of 0.03 (carbon), 5.32 (central nitrogen), and 1.78 eV (imino nitrogen). The central nitrogen atoms were assumed to be equivalent, supplying 1.5 electrons each to the π -system. In addition, σ polarizability was taken into account according to Hammond.^{15c} Resonance integrals were taken to be -2.48 (β_{CN}) and -2.42 eV (β_{CC}).^{15b} Two-center repulsion integrals were computed by the method of Mataga and Nishimoto.^{15d} The choice of configuration was based on energetic considerations, and all singly excited configurations up to 48 393 cm^{-1} were included.

Results and Discussion

The syntheses of CuTAP and CuBoPc were straightforward, although they were obtained as a mixture of four positional isomers. In the case of **1**, eleven components were obtained in the column chromatography as a result of mixed condensation of the two kinds of nitriles (Table 1). Of these, the components (a), (b), (d), and (e) were considered to be isomers of CuTAP without carrying out mass analysis since their Q and Soret band positions were very close to those of CuTAP (583 and 337 nm, respectively, in pyridine as a mixture of isomers).¹¹ Since the mass spectrum of the most abundant component (d) showed the desired parent ion peak at m^+/z 600, this was used for various experiments. From the Q-band position of 614 nm, the component (f) was considered to be an isomer of the copper

complex of TAP fused with one benzene unit. Having a parent ion peak at m^+/z 1370, this species was identified as compound **2** in Figure 1. Based on the Q-band peak positions of around 640 nm, the components (c) and (g)–(i) were considered to be the isomers of **1**. However, the components (g) and (h) were not fragmented in the mass analysis, and since the components (i) and (j) gave the desired parent ion peak at m^+/z 770, the more abundant component (i) was chosen to use in the experiments below.

Figure 2 shows the electronic absorption and magnetic circular dichroism (MCD) spectra of **1** in chloroform, together with those of CuTAP and CuBoPc. Due to the smaller and larger π -systems compared to those of Pcs and TAPs, respectively, the Q-band position (633 nm) lies approximately midway between those of normal Pcs (ca. 650–730 nm)^{4,16} and TAPs,⁴ and its intensity is close to the average value of those of the two analogues. The position of the so-called Soret band is analogous to those of normal TAPs.⁴ The bandwidth of the Soret band increases with increasing size of the π -system. In the MCD spectra, dispersion type Faraday A terms were detected corresponding to the absorption peaks in both the Soret and Q-band regions, indicating that their excited states are orbitally doubly degenerate.¹⁶ Here again, the intensity of the Q-band is midway between that of typical TAPs and Pcs.

To confirm our interpretation of the spectrum of **1**, the molecular orbitals of the dianion of **1** were calculated within the framework of the PPP approximation^{15a} using standard Pc X-ray data as the basis for the structure (of course, two benzene units were removed).¹⁴ For comparison, the MOs of the dianions of TAP and Pc were also calculated. The parameters used were the same as those we used in our previous publications.^{6,17} The calculations predicted the Q and Soret bands at 607 and 328

(14) (a) Robertson, J. M.; Woodward, I. *J. Chem. Soc.* **1937**, 217. (b) Barrett, P. A.; Dent, C. E.; Linstead, R. P. *J. Chem. Soc.* **1936**, 1719. (c) Brown, C. J. *J. Chem. Soc. A* **1968**, 2488, 2494. (d) Kirner, J. E.; Dow, W.; Scheidt, J. R. *Inorg. Chem.* **1976**, *15*, 1685.
(15) (a) Pariser, R.; Parr, R. G. *J. Chem. Phys.* **1953**, *21*, 466, 767. Pople, J. A. *Trans. Faraday Soc.* **1953**, *46*, 1375. (b) Tokita, S.; Matsuoka, K.; Kogo, Y.; Kihara, K. *Molecular Design of Functional Dyes: The PPP Method and Its Application*; Maruzen: Tokyo, 1990. (c) Hammond, H. *Theo. Chim. Acta* **1970**, *18*, 239. (d) Mataga, N.; Nishimoto, K. *Z. Phys. Chem. (Frankfurt am Main)* **1957**, *13*, 140.

(16) Stillman, M. J.; Nyokong, T. In *Phthalocyanines: Properties and Applications*; Leznoff, C. C., Lever, A. B. P., Eds.; VCH: Weinheim, Germany, 1989; Vol. I, Chapter 3.
(17) (a) Kobayashi, N.; Lam, H.; Nevin, W. A.; Janda, P.; Leznoff, C. C.; Monden, A.; Koyama, T.; Shirai, H. *J. Am. Chem. Soc.* **1994**, *116*, 879. (b) Kobayashi, N.; Ashida, T.; Osa, T.; Konami, H. *Inorg. Chem.* **1994**, *33*, 1735. (c) Kobayashi, N.; Togashi, M.; Osa, T.; Ishii, K.; Yamauchi, S.; Hino, H. *J. Am. Chem. Soc.* **1996**, *118*, 1073.

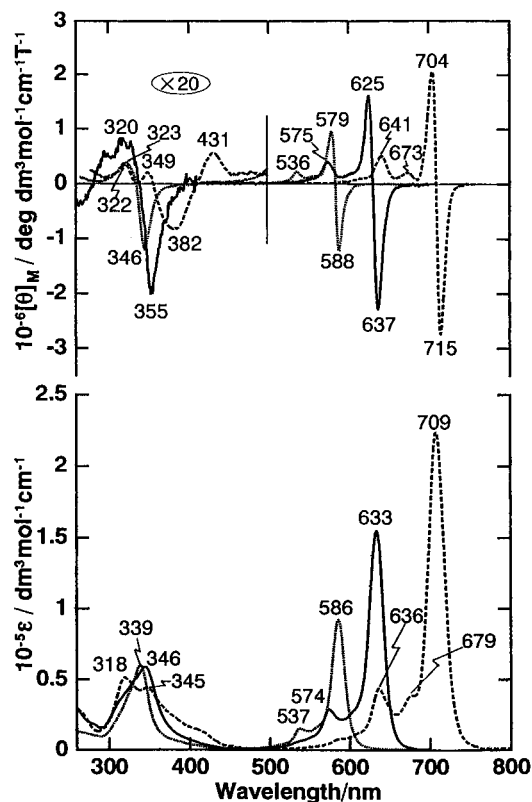


Figure 2. Electronic absorption (bottom) and magnetic circular dichroism (top) spectra of CuTAP, **1**, and CuBoPc in chloroform. The applied magnetic field was 1.09 T.

Table 2. Calculated Transition Energies, Oscillator Strength (f), and Configurations for Compound $\mathbf{1}^{2-}$ and TAP^{2-} ^a

energy/eV	(nm)	f	configurations ^b		
For $\mathbf{1}^{2-}$					
2.016	(615)	0.51	17→18(82%)	16→19(18%)	
2.074	(599)	0.51	17→19(83%)	16→18(17%)	
3.458	(358)	0.20	17→20(84%)		
3.592	(345)	1.04	14→18(36%)	16→18(33%)	15→19(10%)
3.613	(343)	0.72	15→18(41%)	16→19(18%)	14→19(16%)
			17→20(14%)		
3.779	(328)	1.40	14→18(43%)	16→18(38%)	
3.779	(328)	1.27	15→18(42%)	16→19(36%)	
4.073	(304)	0.28	12→19(62%)	11→18(20%)	
4.099	(303)	0.53	11→19(43%)	13→19(20%)	12→18(18%)
For TAP^{2-}					
2.093	(592)	0.21	13→14(72%)	12→15(28%)	
2.093	(592)	0.21	13→15(72%)	12→14(28%)	
3.531	(351)	0.72	8→14(36%)	11→14(28%)	12→14(16%)
			13→15(11%)		
3.531	(351)	0.72	8→15(36%)	11→15(28%)	12→15(16%)
			13→14(11%)		
3.908	(317)	2.17	13→14(45%)	13→15(28%)	12→15(15%)
3.908	(317)	2.17	13→15(45%)	13→14(28%)	12→14(15%)
4.039	(307)	0.34	12→15(56%)	12→14(39%)	
4.093	(307)	0.34	12→14(56%)	12→15(39%)	

^a Excited states with less than 4.1 eV and f greater than 0.20 are shown. ^b Orbital numbers of 17 and 13 are HOMOs of $\mathbf{1}^{2-}$ and TAP^{2-} , respectively.

nm, respectively (Table 2). Since those of Pc and TAP are predicted at 662 and 332 nm and 592 and 317 nm, respectively, the calculations reproduce the trends in the experimental data, although the estimated wavelengths are slightly shorter than the experimental results.¹⁸ In the case of compounds with D_{4h} symmetry such as MtPc and MtTAP, the lowest excited states

are orbitally doubly degenerate so that the HOMO–LUMO transitions are doubly strengthened by the superimposition of two transitions occurring at the same position.^{6,16} The π -conjugated system of **1** has C_{2v} symmetry. However, the appearance of a single Q-band and that of a distinctive Faraday A term at the Q-band in the electronic absorption and MCD spectra, respectively, suggests that the transition is orbitally doubly degenerate, similar to those in normal D_{4h} π -systems. This is, however, rather surprising because any excited states cannot be degenerate in C_{2v} systems in a strict sense (except for spin-degeneracy). Such a single Q-band for C_{2v} π -systems has been reported for a similar but larger *adjacent* π -conjugating system and has been explained by the symmetry-adapted perturbation (SAP) method.⁶ It was concluded that this type of symmetry-lowering effect worked as less significant terms in the higher order perturbations and that consequently only a shift of the Q-band was observed without detectable energy splitting. The appearance of a single Q-band for the dibenzoTAP in this study can be explained in the same manner. Although it is still unknown why a Faraday A term appears at the Q-band, irrespective of the lack of a symmetry element higher than 3-fold rotation axes, this may be similarly understood within the precision of the first-order perturbation (note that both the SAP and Zeeman effects are first-order perturbations). The MO calculation results (Table 2) predict a Q-band split for this system. However, this is not surprising since the PPP calculation was done based on the actual C_{2v} symmetry and included up to much higher perturbation terms than the SAP method, the effects of which may have been overestimated. We should note that even the calculation based on C_{2v} symmetry predicts the appearance of two transitions which are close in energy and have the same intensity (Table 2). Accordingly, two transitions of equal intensity contribute to the Q-band of **1**. The calculated Q-band intensity increases with increasing molecular size, i.e. the oscillator strength (f) (the sum of those of the lowest two transitions) increases from 0.42 of TAP to 1.02 of **1** and further to 1.68 of Pc. The Soret band region is complex because all bands are mixtures of several configurations.^{6,16} There is, however, little difference in the total intensity in the Soret region, i.e. $f = 4.34, 4.43,$ and 4.38 in the above compounds' order. These general features are observed in the experimental data (Figure 2). Checking the configuration of the Q-bands, they are roughly expressed by an one-electron description, but their "purity" increases with increasing molecular size, i.e. the ratio of HOMO–LUMO (and also to LUMO+1 in the case of **1**) transition contribution varies from 72% for TAP to 82% for **1** and further to 87% for Pc. The residue in **1** is a contribution from HOMO–1-to-LUMO and HOMO–1-to-LUMO+1 transitions.

The spectrum of compound **2** is shown in Figure 4A. The somewhat broader Q and Soret bands appear at 614 and 341 nm, respectively. The position of the former band is shifted to the red compared with that (586 nm) of CuTAP but is shorter wavelength than that of **1** (633 nm) which has two fused benzene units. Since the π -conjugated system of **2** is C_{2v} in symmetry, a split Q-band is expected.⁶ The lack of explicit splitting

(18) The wavelength difference between the calculation and experiment is ca. 25–26 nm for compound **1**. Of this difference, approximately 13–16 nm are attributable to the substituent effect of two ether linkages and ca. 3 nm are due to two *tert*-butyl groups (see refs 12 and 17b). Accordingly, the *adjacent* dibenzoTAP without substituent groups may show the Q-band at ca. 614–617 nm. The calculated Q-band position (607 nm) appears, therefore, not markedly short compared with the actual systems. In a similar manner, monobenzo-fused TAP without substituents may show a Q-band at ca. 601–603 nm, since compound **2** has a Q-band at 614 nm.

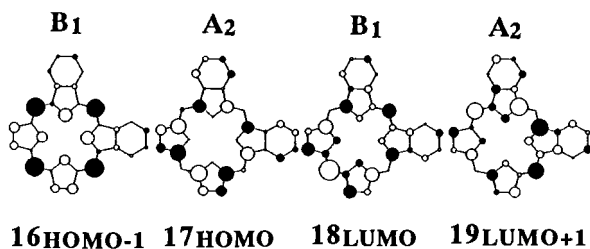


Figure 3. Four frontier orbitals of adjacent dibenzotetraazaporphyrin dianion.

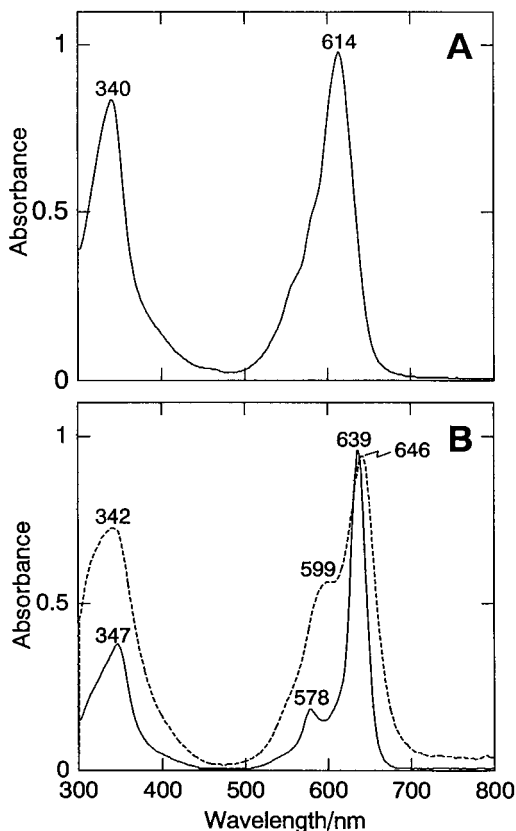


Figure 4. Electronic absorption spectra of (A) compound **2** in chloroform and (B) **1** in chloroform (solid line) and as a film (broken line). Film was obtained by evaporating chloroform in a cell.

therefore inversely implies that the splitting is small. According to SAP theory,⁶ the magnitude of shift of a Q-band to the longer wavelength accompanying the fusion of aromatic moieties parallels the number of aromatic units. Therefore, the energy difference between the Q-band of CuTAP and that of **2** is expected to be approximately the same as that between compounds **2** and **1**. Indeed, the observed values are ca. 780 and 490 cm^{-1} , respectively. Taking into consideration the effect of the substituent groups, these values seem reasonable.¹⁸

In Figure 4B, the absorption spectra of **1** in chloroform and in the form of a film are being compared. For phthalocyanines, upon film formation, it is known¹⁹ that the Q-bands of Pcs with alkyl or alkoxy groups attached to the benzene carbons furthest from the Pc core lie to the blue compared to the same Pcs in solutions, while Pcs with eight alkoxy groups closest to the Pc have a Q-band shifted to the red.²⁰ For phthalocyanines, this information has been important in designing applications, for example, for optical disks. In the case of dibenzoTAPs, no such

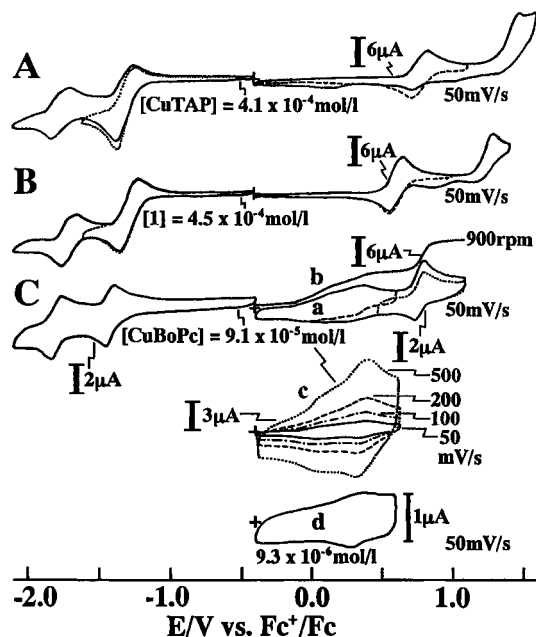


Figure 5. Cyclic (and partly rotating-disk electrode) voltammograms of (A) CuTAP, (B) **1**, and (C) CuBoPc in CH_2Cl_2 with 0.1 M TBAF₆. Concentrations of each compound and the scan rates for each voltammogram are shown.

Table 3. Redox Potential Data (vs Fc^+/Fc) for CuTAP, **1**, and CuBoPc in CH_2Cl_2 Containing 0.1 M TBAF₆^a

species	2nd oxid.	1st oxid.	1st redn.	2nd redn.
CuTAP	1.41(100) ^b	0.76(70)	-1.31(110)	-1.74(120)
1	1.23 (90) ^b	0.61(80)	-1.28(110)	-1.70(110) ^d
CuBoPc	0.79 (60) ^b	0.32(80) ^c	-1.38 (60)	-1.77 (70)

^a Numbers in parentheses indicate the potential differences, ΔE_p , between cathodic and anodic peak potentials at a sweep rate of 50 mV/s. ^b Irreversible wave due to the chemical instability of the electrogenerated species. ^c Quite often, as mentioned in text, a prewave is observed at 0.08 V with $\Delta E_p = \text{ca. } 50$ mV. This couple diminishes with the lowering of [CuBoPc] and the increase of sweep rate. We assigned this wave, therefore, to a dimer or higher aggregates. ^d At slower scan rate, the reoxidation peak splits into two.

information has been reported to date. As seen in this figure, the Q-band of **1** shifted to the red by 4–5 nm while the Soret band shifted to the blue by ca. 6 nm on film formation. Further data are required to obtain general conclusions on the film spectra of dibenzo-substituted TAPs.

Figure 5 shows the cyclic voltammograms of CuTAP, **1**, and CuBoPc, and some electrochemical data are summarized in Table 3. In all cases, two reduction and two oxidation couples were observed. The first oxidation and reduction couples of CuTAP and **1** are reversible if the potential sweeps are switched before reaching the second oxidation and reduction. Based on their peak-to-peak potential separation, ΔE_p , values, all of the couples except the first oxidation of CuBoPc are one-electron processes. Although the first oxidation couple of CuBoPc alone appears to be rather broadened, approximately the same amount of limited current is observed for the first and second oxidation couples in the RDE voltammogram (curve b), indicating that the first oxidation couple is also a one-electron process. Since the central copper ions are not involved in the electron-transfer

(19) Kobayashi, N.; Higashi, R.; Tomura, T. *Bull. Chem. Soc. Jpn.* **1997**, *70*, 2693.

(20) For example, 4,4',4'',4'''-tetra-*tert*-butylated CuPc in chloroform and its solvent-evaporated film show a Q-band at 680 and 618 nm, respectively, while the Q-band of 1,4,11,15,18,22,25-octabutyl CdPc in CHCl_3 and its film appear at 734 and 738 nm, respectively (our unpublished data).

over this potential range, all the redox processes are assigned as ligand-centered. In particular, the assignment of the first oxidation couples has been confirmed spectroelectrochemically (see below). Careful inspection of the first oxidation wave of CuBoPc found that the wave was composed of two overlapping waves (curve a). Such a double wave is often observed in the oxidation of strongly aggregated MtPcs²¹ and can be understood if we assume the presence of aggregation–disaggregation equilibrium for both of unoxidized and oxidized species.^{21a} That is, CuBoPc monomer and dimer (or higher aggregates) are oxidized at the more anodic and less anodic parts of the double wave, respectively, to form the corresponding ring-oxidized species. The assignment of the monomer wave is easily confirmed by the prominence of the more anodic wave in a more dilute solution (curve d). The monomer dimerizes at a given kinetic rate upon ring-oxidation (note that it is known that ring-oxidized MtPcs tend to aggregate more strongly than unoxidized species^{22,23}). If this speculation is correct, the oxidized monomer will be rereduced as it is still in monomer form when we scan the applied potential fast enough before it dimerizes, but it will be rereduced as a dimer at slower scans. This has been supported by cyclic voltammograms at various scan rates (curves c): of the two couples, the rereduction wave at more anodic potential (about 0.3 V) became more prominent at faster scans while the less anodic counterpart diminished.

The redox potentials of the three compounds in this study are summarized in Table 3. The data clearly indicate that oxidation potentials change negatively with increasing molecular size, while the reduction potentials differ only slightly for the different species. This kind of phenomenon has already been reported for Pc and Pc analogues^{6a,11,17b} and, since no redox couple of copper is involved, indicates that the HOMO level destabilizes while the LUMO level remains almost constant on expansion of the π -systems. The redox couples of CuBoPc should be shifted negatively by the presence of the four ether oxygens attached to benzene carbon atoms closest to the Pc core. Therefore, this may be the reason that its first and second reduction potentials appeared at more negative potentials than the corresponding potentials of compound **1**. However, the potential difference, ΔE , between the first oxidation and reduction decreased from 2.07 V in the case of CuTAP to 1.89 V of compound **1** and further to 1.70 V for CuBoPc. Since these ΔE values for CuTAP and CuBoPc are typical of those for TAPs¹¹ and Pcs,²⁴ the value ($\Delta E = 1.89$ V) obtained for compound **1** may also be a reasonable value for *adjacent* dibenzo-substituted TAPs. The ΔE value between the first and second reduction potentials, on the other hand, does not differ markedly between the three species (0.43, 0.42, and 0.39 V for CuTAP, compound **1**, and CuBoPc, respectively). With respect to the above experimental data, the tendency for only the first oxidation and reduction to change is approximately reproduced by the molecular orbital calculations as follows. The energies of the LUMO+1 MO and LUMOs, HOMO, and HOMO–1 MOs in eV are estimated as follows for the deprotonated π -systems in this study; TAP²⁻, –2.6154, –4.1540, –8.5549, and –9.5493; adjacent dibenzoTAP²⁻ (i.e. **1**²⁻), –2.3785, –3.8911, –8.0237, and –9.5445; Pc²⁻, –2.2038, –3.7442,

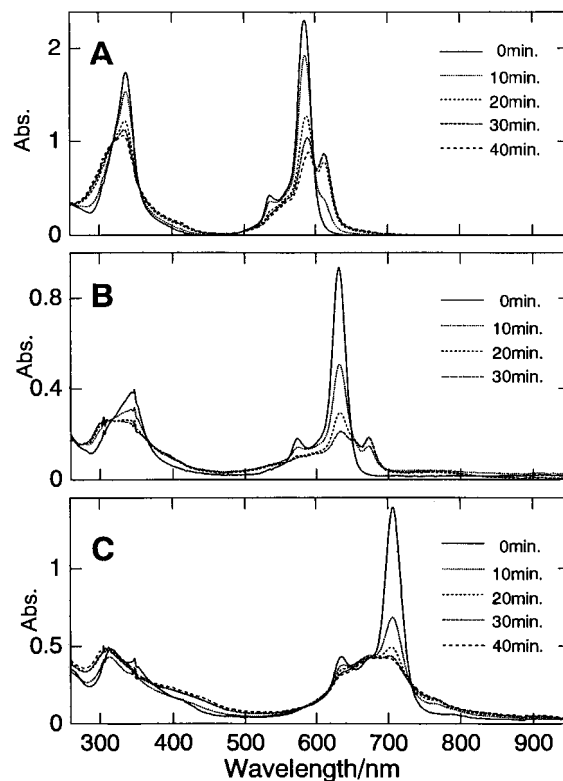


Figure 6. Spectroscopic changes observed in the process from (A) CuTAP, (B) compound **1**, or (C) CuBoPc to their monocationic species in an LOTTLE.⁹ The solvent was CH₂Cl₂ containing 0.2 M of TBAPF₆. The applied potentials were 1.0, 0.9, and 0.6 V vs Fc⁺/Fc couple for CuTAP, compound **1**, and CuBoPc system, respectively.

–7.4869, and –9.5805. Of these, the value of –3.8911 is the average of –3.8892 and –3.8930. From these values, the destabilization of the HOMO level is calculated to be 1.068 eV on going from TAP²⁻ to **1**²⁻ and further to Pc²⁻, while that of the first LUMO level is approximately 0.40 eV. The large destabilization of the HOMO level is in accord with the negative shift of the first oxidation potential on ring expansion, while the much smaller destabilization of the LUMO level accords with the lower sensitivity of the first ring reduction potential to the size of the π -systems.

Figure 6 shows the spectral changes for TAP, **1**, and Pc during the electrochemical oxidations at the 200 mV positive of the first oxidation waves. In all cases, the prominent Q-bands of the initial species decrease in intensity while new absorption bands grow to the red as the oxidations proceed. In addition, the original Soret bands of the initial species diminish and the absorbance at both the blue and red sides increases slightly. In addition, the bands become less sharp with expansion of the π -conjugation system. The spectral changes were fully reversible and the initial spectra were reproduced upon electrochemical rereductions. On the basis of the drastic spectral changes both in peak positions and intensities and the reversibility of the spectral changes, the first oxidation couples for all the three species have been assigned as chromophore-centered. It is rather surprising that the one-electron-oxidized CuPc did not show a prominent absorption band at around 500 nm, which is a “fingerprint marker band” of ring-oxidized Pcs,²⁵ i.e., MtPcs(–1)⁺.²⁶ The possibility that our new spectroelectrochemical cell worked improperly has been completely excluded because

(21) (a) Isago, H.; Leznoff, C. C.; Ryan, M. F.; Metcalfe, R. A.; Davids, R.; Lever, A. B. P. *Bull. Chem. Soc. Jpn.* **1998**, *71*, 1039. (b) Bernstein, P. A.; and Lever, A. B. P.; *Inorg. Chem.* **1990**, *29*, 608.
 (22) (a) Homborg, H.; Kalz, W. Z. *Naturforsch., Sect. B* **1978**, *33*, 1067. (b) Homborg, H. Z. *Anorg. Allg. Chem.* **1983**, *507*, 35.
 (23) Ough, E.; Gasyana, Z.; Stillman, M. J. *Inorg. Chem.* **1991**, *30*, 2301.
 (24) Lever, A. B. P.; Milaeva, E. R.; Speier, G. In *Phthalocyanines: Properties and Applications*; Leznoff, C. C., Lever, A. B. P., Eds.; VCH: Weinheim, Germany, 1993; Vol. III, Chapter 1.

(25) Stillman, M. J. In *Phthalocyanines: Properties and Applications*; Leznoff, C. C., Lever, A. B. P., Eds.; VCH: Weinheim, Germany, 1993; Vol. III, Chapter 5.

preliminary experiments on the electrochemical oxidation of ZnPc under the same conditions gave rise to normal spectral changes characteristic of $\text{ZnPc}(-1)^+$ formation.²⁷ One plausible explanation is that the electrogenerated species aggregates very strongly, so that the aggregated species may produce such an unusual spectrum. The aggregation of the oxidized CuBoPc has been supported by the cyclic voltammetry experiments (see above). Since a bulk electrolysis gives the generated species enough time to aggregate upon oxidation compared to cyclic voltammetry, it is reasonable to assume that all the bulk species will aggregate on this time scale. Electronic absorption spectra of both monomeric and dimeric $\text{MtPc}(-1)^+$ species are known and there are some differences between them.²⁵ The most prominent changes upon dimerization are the disappearance of a peak at around 800–850 nm and the simultaneous growth of a new absorption band, the latter of which is quite often observed as a very broad and ill-defined band,²⁸ at the tail of the longer wavelength side of the Q-band of the unoxidized species.^{23,27,29} Based on the absence of a sharp peak in the 800–850 nm region and the appearance of very broad band at around 750–800 nm (Figure 6c), the oxidized CuBoPc is likely to be highly aggregated. It should be noted that one-electron-oxidized porphyrins are known to be prone to dimerization.²⁹ With this taken into consideration, a careful inspection of the CuBoPc- $(-1)^+$ spectrum found a broad absorption band in the 380–480 nm range. This band may correspond to the fingerprint marker band of $\text{MtPc}(-1)^+$, since the absorption band of aggregated Pcs appears at shorter wavelength than that of monomers and Pcs with alkoxy groups attached closest to the Pc core often show broad bands in 250–500 nm.¹²

As far as we know, no published electronic spectral data for ring-oxidized TAP or dibenzoTAP have been available. Hence this is the first article to report this kind of data. Unlike the normal $\text{MtPc}(-1)^+$ species, neither of the ring-oxidized TAP nor dibenzoTAP showed the fingerprint marker band in 500–550 nm region. Since the origin of this marker band is unknown

(although some suggestions have been proposed), it is unclear whether such a band exists for these species. It is noteworthy that the absence of the marker band was quite recently reported also for the one-electron-oxidized species of octaethylTAP and its zinc complex.³⁰

The thermal stability of compound **1** was checked by TGA. The initial decomposition temperature, flexion temperature, and maximum decomposition temperature are 197.1, 410.5, and 415.9 °C, respectively. Since the corresponding values for 4,4',4'',4'''-tetra-*tert*-butylCuPc are 432.1, 489.7, and 511.0 °C, respectively,³¹ this result indicates that the decomposition temperature of compound **1** is about 95 °C lower than that of 4,4',4'',4'''-tetra-*tert*-butylCuPc. On the TGA of compound **1**, the weight loss occurs via three steps. The first, second, and third steps (ca. 5, 13, and 70%, respectively) occurred in ca. 197.1–240, 240–410.5, and above ~410.5 °C. Of these, the one at the last step alone appears to correspond to the decomposition of the *adjacent* dibenzoTAP parent.

Conclusion

An *adjacent* dibenzotetraazaporphyrin was synthesized as a copper complex for the first time and its spectroscopic and electrochemical properties were reported, together with the results of molecular orbital (MO) calculations. The compound showed intermediate characteristics between those of tetraazaporphyrins and phthalocyanines. Thus, in the order of TAP, dibenzoTAP, and Pc, the Q-bands shift to the red and intensify while the Soret band broadens with increasing size of the π -system. In addition, comparison of their redox potential data indicates that the LUMO level remains almost constant while the HOMO level destabilizes with the increase in the size. The spectroscopic properties and redox potentials were reproduced by MO calculations within the framework of the PPP approximation. The positions of the Soret and Q-bands of the *adjacent* dibenzotetraazaporphyrin are not significantly shifted from those in solution on film formation. Thermogravimetric analysis suggested that the skeleton of the *adjacent* dibenzotetraazaporphyrin is thermally weaker than the corresponding Pc skeleton by ca. 100 °C.

Acknowledgment. We thank the Mitsubishi Foundation for financial support and Dr. H. Konami for his help in MO calculations.

IC9806535

- (26) The Pc unit is an 18π electron system that, in its common oxidation state, carries two negative charges. This is designated $\text{Pc}(-2)$. This unit is capable of oxidation or reduction. Thus oxidation by one electron yields $\text{Pc}(-1)^+$. Similarly, the oxidation product of TAP by one electron is designated $\text{TAP}(-1)^+$.
- (27) (a) Nyokong, T.; Gasyna, S.; Stillman, M. J. *Inorg. Chem.* **1987**, *26*, 1087. (b) Mack, J.; Stillman, M. J. *J. Phys. Chem.* **1995**, *99*, 7935.
- (28) (a) Nevin, W. A.; Lever, A. B. P. *Anal. Chem.* **1988**, *60*, 727. (b) Manvannan, V.; Nevin, W. A.; Leznoff, C. C.; Lever, A. B. P. *J. Coord. Chem.* **1988**, *19*, 139.
- (29) (a) Song, H.; Reed, C. A.; Scheidt, W. R. *J. Am. Chem. Soc.* **1989**, *111*, 6865. (b) Schulz, C. E.; Song, H.; Mislanker, A.; Orosz, R. D.; Reed, C. A.; Debrunner, P. G.; Scheidt, W. R. *Inorg. Chem.* **1997**, *36*, 406.

(30) Kaga, N.; Ishikawa, N.; Kaizu, Y. In *Abstracts of the 72nd Annual Meeting of CSJ*, Tokyo, 1997; Abstract No. IC102.

(31) Liu, Y. Q.; Zhu, D. B. *Synth. Met.* **1995**, *71*, 1853.